AFRL-VA-WP-TP-2002-329

REACTIVE FLOW CONTROL SYSTEM USING INTELLIGENT CONTROL MODULES FOR VIRTUAL AERODYNAMIC SHAPING

Mehul P. Patel
Troy S. Prince
Richard M. Kolacinski
T. Terry Ng
Alan B. Cain

DECEMBER 2002

THIS IS A SMALL BUSINESS INNOVATION RESEARCH (SBIR) PHASE 1 REPORT

Approved for public release; distribution is unlimited.

AIR VEHICLES DIRECTORATE
AIR FORCE RESEARCH LABORATORY
AIR FORCE MATERIEL COMMAND
WRIGHT-PATTERSON AIR FORCE BASE, OH 45433-7542

REPORT DOCUMENTATION PAGE

Form Approved
OMB No. 0704-0188

1. REPORT DATE *(DD-MM-YY)*	2. REPORT TYPE	3. DATES COVERED *(From - To)*
December 2002	Conference Paper Preprint	

4. TITLE AND SUBTITLE

REACTIVE FLOW CONTROL SYSTEM USING INTELLIGENT CONTROL MODULES FOR VIRTUAL AERODYNAMIC SHAPING

5a. CONTRACT NUMBER
F33615-02-M-3227

5b. GRANT NUMBER

5c. PROGRAM ELEMENT NUMBER
65502F

6. AUTHOR(S)

Mehul P. Patel, Troy S. Prince, and Richard M. Kolacinski (Orbital Research Inc.)
T. Terry Ng (The University of Toledo)
Alan B. Cain (Innovative Technology Applications Company)

5d. PROJECT NUMBER
3005

5e. TASK NUMBER
30

5f. WORK UNIT NUMBER
9K

7. PERFORMING ORGANIZATION NAME(S) AND ADDRESS(ES)

Orbital Research Inc.
673G Alpha Dr.
Cleveland, OH 44143

Dept. of Mechanical, Industrial, and Manufacturing Engineering
The University of Toledo
Toledo, OH 43606

Innovative Technology Applications Company
Chesterfield, MO 63006

8. PERFORMING ORGANIZATION REPORT NUMBER

9. SPONSORING/MONITORING AGENCY NAME(S) AND ADDRESS(ES)

Air Vehicles Directorate
Air Force Research Laboratory
Air Force Materiel Command
Wright-Patterson Air Force Base, OH 45433-7542

10. SPONSORING/MONITORING AGENCY ACRONYM(S)
AFRL/VACA

11. SPONSORING/MONITORING AGENCY REPORT NUMBER(S)
AFRL-VA-WP-TP-2002-329

12. DISTRIBUTION/AVAILABILITY STATEMENT
Approved for public release; distribution is unlimited.

13. SUPPLEMENTARY NOTES

This is a Small Business Innovation Research (SBIR) Phase 1 report.

AIAA Applied Aerodynamics Conference presentation, Orlando, FL, June 23-26 2003.

14. ABSTRACT *(Maximum 200 Words)*

A proof-of-concept closed-loop reactive flow control methodology using discrete intelligent control modules for virtual aerodynamic shaping of air vehicles is developed. Discrete suction control technique integrated with dynamic pressure sensors and a closed-loop controller forms the basis of the intelligent control modules, which are then coordinated by a higher-level controller to enable a desired flow effect on the surface of the air vehicle.

15. SUBJECT TERMS

16. SECURITY CLASSIFICATION OF:			17. LIMITATION OF ABSTRACT:	18. NUMBER OF PAGES	19a. NAME OF RESPONSIBLE PERSON (Monitor)
a. REPORT	b. ABSTRACT	c. THIS PAGE			James Myatt
Unclassified	Unclassified	Unclassified	SAR	24	19b. TELEPHONE NUMBER *(Include Area Code)* (937) 255-8491

Standard Form 298 (Rev. 8-98)
Prescribed by ANSI Std. Z39-18

AIAA draft paper
21st AIAA Applied Aerodynamics Conference, Orlando, Florida, 23-26 June 2003

REACTIVE FLOW CONTROL SYSTEM USING INTELLIGENT CONTROL MODULES FOR VIRTUAL AERODYNAMIC SHAPING

Mehul P. Patel,* Troy S. Prince,† and Richard M. Kolacinski,‡
Orbital Research Inc., Cleveland, OH 44143

T. Terry Ng§
Dept. of Mechanical, Industrial, and Manufacturing Engineering
The University of Toledo, Toledo, OH 43606

and

Alan B. Cain**
Innovative Technology Applications Company
Chesterfield, MO 63006

Abstract

A proof-of-concept closed-loop reactive flow control methodology using discrete intelligent control modules for virtual aerodynamic shaping of air vehicles is developed. Discrete suction control technique integrated with dynamic pressure sensors and a closed-loop controller forms the basis of the intelligent control modules, which are then coordinated by a higher-level controller to enable a desired flow effect on the surface of the air vehicle. Static and dynamic wind tunnel tests at Mach 0.08 on a two-dimensional airfoil with discrete suction control embedded via a series of holes on the upper surface near the trailing edge has been conducted. Apart from increased aerodynamic efficiency using discrete suction control, information about timescales related to the actuator response time and the flow dynamics time is obtained from a series of dynamic tests for both, constant alpha and pitching maneuvers. Data from these static tests, dynamic tests and computational studies is being used to develop a closed-loop control algorithm to form the basis of the intelligent control module operation. A number of intelligent control modules located discretely on the surface of the air vehicle will then be coordinated by a higher level controller enabling a desired maneuver of the air vehicle. A collaborative effort to demonstrate the effectiveness of the prototype system via experimental and computational studies is under way.

Introduction

Combat arenas in the near future will require unprecedented levels of performance from air vehicles to meet mission-specific objectives. Future air vehicles will need to be highly maneuverable, stealthy, and reliable. To meet these requirements from an aerodynamic point of view, the future UAVs will need to be able to maintain its ability to control and maneuver without the use of the conventional hinged control surfaces. Furthermore, some air vehicles may need to be designed with non-aerodynamic surfaces to carry specific types of sensors and armament. Advanced control techniques are necessary to enable these new air vehicles.

Reactive Flow Control is designed to render the revolutionary capability to virtually aerodynamically shape air vehicles. Virtual shaping of aerodynamic surfaces causes the flow field to behave as if it is encountering geometry different from the actual surface. Virtual aerodynamic shaping has the potential to enable completely revolutionary air vehicle designs such as vehicle designed around the requirements of a sensor rather than aerodynamics or by the reduction or elimination of hinged control surfaces. This capability can result in higher lift to drag ratio with increased maneuverability and lower fuel consumption.

To enable a reactive flow control system to be implemented on an air vehicle, it is necessary to incorporate a number of key components. These components can be classified into sensors, actuators, and control loop. All three of these elements then must be designed and packaged to enable easy integration

* Senior Aerodynamicist, Member AIAA
† Vice President of Technology, Member AIAA
‡ Director of Controls Engineering
§ Professor, Senior Member AIAA
** President, Associate Fellow AIAA

into the airframe with minimal space requirements, minimal connections required and easy field replaceability. Specific features and highlights of each of these components are discussed below.

Flow Control Work

In recent years, the advent of smart actuators based on technologies such as piezoelectric materials, MEMS, and shape memory alloy (SMA) has led to the development of various devices to provide control to the aircraft by altering local aerodynamic flow phenomena. The most significant characteristic of these devices is the ability to induce concentrated inputs of energy at critical locations in the flowfields to manipulate the flow over the surface for a desired effect. This enables the concept of an adaptive virtual aerodynamic surface that can be tailored to different operating conditions. One of the potential applications of such technology is in the development of UAVs without conventional control surfaces for maneuverability with low observability, reduced drag and weight, and design flexibility. Furthermore, this technology is a logical application to the air vehicle where the functional requirements dictate a non-aerodynamic shape. As such, a significant improvement in the aerodynamic control and efficiency are needed and can be obtained through active flow control.

Examples of current active flow control devices include, among others, the zero-net mass synthetic jet developed by Glezer and co-workers at Georgia Tech[1], pulsed slot blowing by Wygnanski and co-workers at the University of Arizona[2], deployable vortex generators by Orbital Research[3], vortex-generating jets by Physical Sciences Inc.[4], and discrete suction by Ng at the University of Toledo[5]. While the basic principles behind these controls can be quite different, they all share one thing in common in that one of their main functions is *separation control.* The main advantage of a separation-based control is that very large control forces can be generated using devices that are potentially smaller in size, lower in weight, and less mechanically complex than other controls such as a variable-camber airfoil. Additional to separation control, there are a few other concepts such as variable-camber airfoils and microtabs[6] (at proof-of-concept stage at UC-Davis) that are based on camber control to change the lift. In general, the success of these concepts depends on reliable actuators and control strategies that need to be developed.

Flow Sensing

Sensor information is critical to the design of a closed-loop flow control system since it provides crucial information on the sub-layer flow field required for the design and tuning of the closed loop feedback controller. Practical sensors for flow control systems need to be both robust and not alter the flow field they are measuring. To prevent interactions with the airflow, the sensors must be flush mounted with the aerodynamic surface. Therefore, sensors for active flow control techniques are typically limited to either dynamic pressure or sheer stress.

Previous flow control research by Orbital Research Inc. has led to the development of a closed-loop separation control system based on a mathematical model that utilizes the distinctive nature of pressure fluctuations indicative of flow separation.[7] It was shown that a single pressure sensor could be used for detection flow separation and thereby detecting wing stall, if located optimally. This technique is a potential candidate for the detection of abnormal flow behavior to actuate the discrete suction control actuation within each intelligent control module of the reactive flow control system that is currently under investigation.

Closed-Loop Flow Control

Novel aerodynamic flow control techniques provide considerable promises to enable enhanced aircraft performance across a wider range of flight regimes than currently possible. Such unconventional control schemes will enable virtual aerodynamic shaping of air vehicles while increasing the overall control authority and the *stealth-ness.* Open-loop, active flow control techniques have been successfully developed that allow effective control of flow separation. There are however strong reasons for a closed-loop, reactive control. First, vehicle designs meeting a wide range of mission requirements often are susceptible to sudden departures from controller flight. Second, vehicle motions, especially when coupled with unconventional airframe designs, can introduce dynamic flow-field behaviors that are difficult to predict. Additionally, component failure or vehicle damages can render an open-loop system ineffective. Thus besides a reliable and an effective control mechanism, one critical component of the reactive flight control system is the development of a robust feedback controller to close-the-loop for maintaining aerodynamic performance shall the unpredictable occurs.

Real-time closed-loop control models relying on sensors and actuators are an exceptional approach to the control of unsteady aerodynamics. Advancements in micro-machining technology have revolutionized the

capabilities of these controls. Various theoretical and CFD software have been aimed at understanding the boundary layer and separation phenomena ranging from subsonic to supersonic speeds for scheming an effective control model. However, a universal feedback controller based on MEMS sensor/actuator arrays for active flow control has yet not identified.

There have been numerous different approaches to active flow control. There are a number of different model based controller approaches that have been demonstrated with varying degrees of success. A new approach to the development of control algorithms has been based on linearized approximations of the flow state and has resulted in either static optimal control designs or a variety of gain scheduling controllers.[8] Extensive work has also been performed on the development of nonlinear feedback control algorithms based on simplifications of the full non-linear Navier-Stokes equations as well.[9] Other non-traditional control systems have also been used to adaptively find feedback laws to minimize local wall shear stress, such as neural networks.[10] Our concept, still in the development stage, is described in the following sub-sections.

Intelligent Control Modules Approach

The architecture of our closed loop controller is decomposed into two levels, a local controller that controls the amount of lift created by a wing section and a global controller that coordinates the local controllers in order to modulate the net pitch and rolling moments created by the entire wing. For the purposes of this feasibility study, it is assumed that the lift generated by a wing section is independent of the lift generated by all other wing sections. Under this assumption, the lift produced by a wing is the sum of the lift forces generated by the separate wing sections. By modulating the lift generation of the wing sections, the net lift force and the spanwise center of pressure can be modulated independently. The pitching moment is then a linear function of the net lift produced and the rolling moment is a function of the net lift force and the location of the spanwise center of pressure. The global controller modulates the net force and center of pressure location by varying the weighting or influence coefficients of predetermined lift distributions spanwise along the wing. In particular, the lift distribution along the wing is constructed from the superposition of two "shape functions," a constant bias and a linearly varying distribution. Adjusting the weighting of the component shape function then controls the net distribution. Using the shape functions, the global controller essentially specifies a lift to be generated by each of the individual local wing sections. A local controller regulates the lift force generated by the individual wing sections. The lift produced by a wing section is a function of the pressure coefficient over the surface of the wing section. This pressure coefficient may be modulated by the discrete suction technique.

Airfoil Model

A two-dimensional airfoil model with 19.05 cm chord and 30.48 cm span was used for the flow control experiments. Figure 1 shows details of the airfoil model configuration. The model was designed and fabricated using the NC machine at UT. Psi scan modules, force balance stinger and eight dynamic pressure sensors, EPE-83 series from Entran®, were chosen as the sensing elements and used for data acquisition. The pressure sensors were surface-mounted on the airfoil.

Wind Tunnel Testing

Low speed wind tunnel tests were performed at the University of Toledo 3 x 3 ft. closed-loop low-speed wind tunnel for α ranging from -2° to 12° at a R_e number of 0.35 million based on the wing chord length of 19.05 cm. Static and dynamic sweep tests with varying sweep rates were conducted for both the baseline model configuration (no control) and the smart model configuration (with active flow control).

Programs (VI files) were developed using LabView™ to control the on-off states of flow control devices so as to capture enough data points to fully represent the sectional flowfield information during both static and dynamic conditions. Programs to capture the time responses of the actuators during static and dynamic tests were also developed.

Results

Figures 2 and 3 shows the effect of zero-net mass synthetic jet and discrete suction techniques on the pressure distribution over the upper and lower surfaces of the 2-D airfoil for angles of attack ranging from -2° to -8° in 2° increments. Wind tunnel tests were conducted at a R_e number of 0.35 million, based on the wing chord length of 19.05 cm. Both the control techniques were implemented via a series of discrete holes on the surface of the airfoil located toward the trailing edge of the airfoil just after the reflex line. A 2-stroke model engine of 0.25 cubic inches was employed as the signal source, which was swung through compression and rarefaction equally at 60 Hz to simulate a zero-net mass synthetic jet actuator. Suction for discrete suction technique was enabled via a simple suction pump with a variable suction rate control valve.

The suction rate coefficient C_m of 0.00172 was used for the experiments. [Cm = (mass flow rate)/(density of air x freestream velocity x wing area)] For the given test conditions and the hardware configuration, discrete suction was found to be more effective in altering pressure distribution around the airfoil than the synthetic jet actuator.

The discrete suction technique was chosen for the development of the closed-loop flow control strategy. Results from the force modulation experiments conducted for -4° to 6°AoA are presented in Figs.4-9. These tests were conducted to obtain the estimates of magnitude control for varying input states. The input variation (suction rate coefficient) was achieved by the variable suction rate control valve. Dynamic tests for similar angles of attack range at similar flow conditions were conducted in order to obtain the actuator response time and the time constant associated with the flow dynamics. Figure 10 presents a characteristic flowfield response from dynamic sensor 5 (pressure coefficient) as a function of valve state and time. Dynamic experiments were conducted for a range of C_m values and the associated timescales were used for the controller development. Figures 11 and 12 show the zoom-in plots for the control-on and control-off states with typical damping characteristics.

Figures 10 through 12 show the step response of the open loop system at one of the sensor location. Initial examination of the step responses at other sensor locations indicates that the dynamics remain constant over the surface of the wing with only the open loop gain varies. As the lift is computed by an integration of the pressure coefficient over the wing surface, the net lift produced by a wing section may then be assumed to possess the same dynamics and whose open loop gain is then the integral of the open loop gain over the wing surface. The entire lift generated by a wing section can then be represented by a single input-output mapping between the suction coefficient and the lift generated. Furthermore, this mapping differs from that shown in Figs. 10-12 only in open loop gain.

A second order model with an integer delay has been chosen to represent this system. The open loop transfer function for this system (without the delay) is,

$$G(s) = \frac{K}{s^2 + 2\xi\omega_n s + \omega_n^2}$$

where K is the open loop gain and ω_n and ξ are the natural frequency and damping ratio of the system, respectively. All of these parameters have been obtained from the open loop step response. Figure 13 shows the open loop step response of this model and Fig. 14 depicts a detail from the open loop step response showing the delay in the model. The delay in the model is significantly smaller than the delay seen in the original system. It is believed that the delay in the original system is primarily an artifact of the length of the tubing used to supply the suction in the experiment and would be significantly shorter in an actual implementation. For this reason, a shorter delay is used in the model.

A digital control system has been chosen for this system. Digital Control Techniques were chosen for the ease it provides for modeling delays and to avoid the difficulties inherent in force feedback systems, namely a lack of derivative information. In addition, a digital implementation provides a model form that can be easily used to design an adaptive controller. A Zero Order Hold (ZOH) model was used to produce a discrete transfer function,

$$G(z) = \frac{z-1}{z} Z\left\{\frac{G(s)}{s}\right\} = \frac{K(Az+B)}{z^2 - 2e^{-\xi\omega_n T}(\cos\omega_n\sqrt{1-\xi^2})z + e^{-2\xi\omega_n T}}$$

where T is the sampling period and

$$A = 1 - e^{-\xi\omega_n T}\cos\omega_n\sqrt{1-\xi^2} - \frac{\xi}{\sqrt{1-\xi^2}} e^{-\xi\omega_n T}\sin\omega_n\sqrt{1-\xi^2}$$

$$B = e^{-2\xi\omega_n T} + \frac{\xi}{\sqrt{1-\xi^2}} e^{-\xi\omega_n T}\sin\omega_n\sqrt{1-\xi^2} - e^{-\xi\omega_n T}\cos\omega_n\sqrt{1-\xi^2}$$

Applying a p step delay to the system produces,

$$G(z) = \frac{K(Az+B)}{z^p(z^2 - 2e^{-\xi\omega_n T}(\cos\omega_n\sqrt{1-\xi^2})z + e^{-2\xi\omega_n T})}.$$

This model is then restated in term of the shift operator, q to yield

$$G(q) = \frac{B(q)}{A(q)} = \frac{b_1 q + b_0}{q^{p+2} + a_{p+1}q^{p+1} + a_p q^p}$$

where the coefficients of q are identical to the coefficients of z. This model is known as an ARMA model where the polynomial $A(q)$ contains Auto-Regressive (AR) information and the polynomial $B(q)$ contains Moving Average (MA) information.

The desired closed loop dynamics are specified in a similar form,

$$G_m(q) = \frac{B_m(q)}{A_m(q)}$$

and the pole placement algorithm can be used to design a feedback regulator of the form,

$$R(q)u(t) = T(q)u_c(t) + S(q)y(t).$$

With this controller, the close loop system can be represented as:

$$y(t) = \frac{BT}{AR+BS}u_c(t) + \frac{BR}{AR+BS}v(t)$$
$$u(t) = \frac{AT}{AR+BS}u_c(t) - \frac{BS}{AR+BS}v(t)$$

and the closed loop characteristic polynomial is therefore:

$$AR + BS = A_o A_m B^+ \quad \text{.....Controller Design}$$

where A_o is the observer and B^+ is the polynomial containing the stable zeros of the open loop system. This is a Diophantine equation (Bezout identity) and can be solved easily in real time.

A controller using a set of desired dynamics identical in form to the original open loop system but with $\omega = \sqrt{2}\omega_n$ and $\xi = 0.6$ with a unity closed loop gain was designed and implemented in Matlab. Figure 15 shows the closed loop step response and Fig. 16 depicts a detail from the step response. Figure 17 shows the control input to the system. The closed loop response shows a significant amount of ringing. The ringing can be eliminated by retuning the controller but at the cost of significant overshoot. As there is a significant amount of noise present in the actual system, it is felt that the ringing is preferable to the overshoot because the settling time required to reach the noise floor is extremely small. This ringing is the result of the system delay and the elimination of a stable but lightly damped zero (hence the implicit cancellation of a lightly damped pole). In the absence of a delay, this controller can be tuned to eliminate overshoot and ringing. A redesign of the structure of the desired closed loop dynamics such that the zero is not cancelled should mitigate this problem. A more robust approach, however, is to implement a predictive adaptive controller to ameliorate the effects of the delay. The design of a predictive, adaptive controller such as the GPC (Generalized Predictive Controller) is similar, requiring only an additional tuning parameter the replacement of the ARMA model with a CARIMA (Controlled Auto-Regressive and Integrated Moving Average) model,

$$A(q^{-1})y(t) = B(q^{-1})u(t) + C(q^{-1})\xi(t)/\Delta$$

where $C(q^{-1})$ is a polynomial, $\xi(t)$ is an uncorrelated random sequence and $\Delta = 1 - q^{-1}$ and is the backwards difference operator. This control algorithm has proven to be very effective for systems with non-zero dead-time.

Using adaptive control techniques has the additional benefit of imbuing the controller with the ability to adapt to changing system dynamics. In particular, the system dynamics are also a function of the angle of attack and free stream velocity. The adaption mechanism allows the controller to effectively regulate the flow control device through out its performance envelope without a deterioration of performance. To this end, a Self-Tuning Regulator will be examined.

In a Self-Tuning Regulator (STR), process parameters are updated and controller parameters are obtained form the solution of a design problem that is solved in real-time. A typical STR block diagram is shown in Fig. 18. This type of regulator can be separated into two loops: the inner (process feedback controller) loop and the outer (recursive parameter estimator/design problem solution) loop. The outer loop is dependent on a least squares estimate, that is used to provide system parameters for the updating of the regulator parameter: The estimated parameter are treated as true system parameters and used to redesign the regulator via the pole placement algorithm described above or via an alternative technique such as LQG design.

Self-tuning control is one way to automate process feedback control and design problem solution on-line. The process model and control design parameters are updated each sampling period, and the STR automatically tunes parameters to achieve the desired close loop system response (Specification). In discrete time, the process can be described in state space form as:

$$x(t+1) = \Phi x(t) + \Gamma u(t)$$
$$y(t) = Cx(t)$$

The Controller design block in Fig. 18 accepts two inputs; a setpoint specification describing desired system output dynamics, and a set of identified parameters describing process state. It then calculates a solution to the underlying design problem and updates the controller parameters indirectly, as shown. Note that results given by the process estimation block are assumed to be perfect estimates, with zero uncertainty in accordance with the certainty equivalence principle. If information regarding the quality of the estimate is available, uncertainty estimates may be used in the design of control parameters. The three elements an STR are discussed below.

The estimation block in Fig. 18 identifies a recursive least squares (RLS) model used by the controller design block. Model parameters are based on

the average behavior of the process, using the least squares criterion: $V(\theta,t)=\frac{1}{2}\sum_{i=1}^{t}\left(y(i)-\varphi^T(i)\theta\right)^2$

where y is the observed variable, $\theta_1^0,\theta_2^0,...,\theta_n^0$ represents the parameter to be determined, and $\varphi_1,\varphi_2...,\varphi_3$ are the regressors, known functions that may be dependent on a third variable. The parameter θ is determined to minimize the least squares criterion. When model parameters vary with time, however, identification should be based on the most recent data, and old data should be discounted because it is not representative of the process anymore. To address this issue, data is exponentially discounted using a "forgetting factor." With a forgetting factor (lambda) incorporated, the criterion becomes $V(\theta,t)=\frac{1}{2}\sum_{i=1}^{t}\lambda^{t-i}\left(y(i)-\varphi^T(i)\theta\right)^2$.

Since adaptive controllers observe systems sequentially, computations are often formulated recursively. If a process is given as $y(i)=\varphi^T(i)\theta^0+e(i)$, where θ^0 is the vector of certain parameters and $\{e(i),i=1,2,...\}$ is a sequence of independent equally distributed random variables with zero mean. A recursive least squares estimation of RLS can be formulated as follows:

If the matrix $\ddot{\mathbf{O}}(t)$ has full rank for all $t\geq t_0$ then, given $\hat{\theta}(t_0)$ and $\hat{\theta}(t_0)P(t_0)=\left(\Phi^T(t_0)\Phi(t_0)\right)^{-1}$ the least squares estimate $\hat{\theta}(t)$ satisfies the recursive equations:

$$\hat{\theta}(t)=\hat{\theta}(t-1)+K(t)\left(y(t)-\varphi^T(t)\hat{\theta}(t-1)\right)$$
$$K(t)=P(t)\varphi(t)=P(t-1)\varphi(t)\left(I+\varphi^T(t)P(t-1)\varphi(t)\right)^{-1}$$
$$P(t)=\left(I-K(t)\varphi^T(t)\right)P(t-1)$$

which can be interpreted as a Kalman filter for the process:

$$\theta(t+1)=\theta(t)$$
$$y(t)=\varphi^T(t)\theta(t)+e(t)$$

Once RLS estimation is completed, model-based tuning proceeds with controller design using the identified model. Pole Placement Design is used to attain desired output dynamics based on the identified system

Conclusions

A proof-of-concept closed-loop reactive flow control methodology using discrete intelligent control modules for virtual aerodynamic shaping of air vehicles is developed. Reactive Flow Control is designed to render the revolutionary capability to virtually aerodynamically shape air vehicles. Virtual aerodynamic shaping has the potential to enable completely revolutionary air vehicle designs such as vehicle designed around the requirements of a sensor rather than aerodynamics or by the reduction or elimination of hinged control surfaces. This capability can result in higher lift to drag ratio with increased maneuverability and lower fuel consumption. The development of closed-loop controller is underway.

References

[1] Smith, B.L. and Glezer, A., 1995 "Jet Vectoring by Synthetic Jet Actuators", Bull. Am. Phys. Soc. 40, pp. 2025.

[2] Wygnanski, I., 1997 "Boundary Layer and Flow Control by Periodic Addition of Momentum", AIAA Paper 97-2117, 4th AIAA Shear Flow Conference, Snowmass, CO.

[3] Patel, Mehul P., Carver Reed, Ng, Terry T., and Lisy, Frederick J., 2002 "Detection and Control of Flow Separation Using Pressure Sensors and Micro-Vortex Generators," AIAA paper 2002-0268.

[4] Magill, J. C. and McManus, K. R., "Control of Dynamic Stall Using Pulsed Vortex Generator Jets," AIAA 98-0675, AIAA 36th Aerospace Sciences Meeting and Exhibit, Reno, NV, Jan. 1998.

[5] Ng, T. T., and Lang, Y. "Shear Layer Instability Induced Separation Control," AIAA Journal, Vol. 37, No. 3, March 1999.

[6] Van Dam, C.P.; Yen, D.T.; Vijgen, P.M.H.W. "Gurney Flap Experiments on Airfoil and Wings," Journal of Aircraft (March-April, 1999):484-486.

[7] Patel, Mehul P., Prince, Troy S., Ng, Terry T., and Lisy, Frederick J., 2002 "Control of Aircraft Stall via Embedded Pressure Sensors and Deployable Flow Effectors," AIAA paper 2002-3170.

[8] Högberg, M., Bewley, T.R., Henningson, D.S., Decentralized Feedback Control and Estimation of Transition in Plane Channel Flow, Journal of Fluid Mechanics, 2001.

[9] Gunzburger, M. D. and Manservisi, S., "Analysis and Approximation of the Velocity Tracking Problem for Navier-Stokes flows with Distributed Control," Siam. J. Numer. Anal., 37:1481-1512, 2000.

[10] Lee, C., Kim, J., Babcock, D., and Goodman, R., 1997 Application of Neural Network to Turbulence Control for Drag Reduction. Phys. Fluids 9(6), 1740-1747.

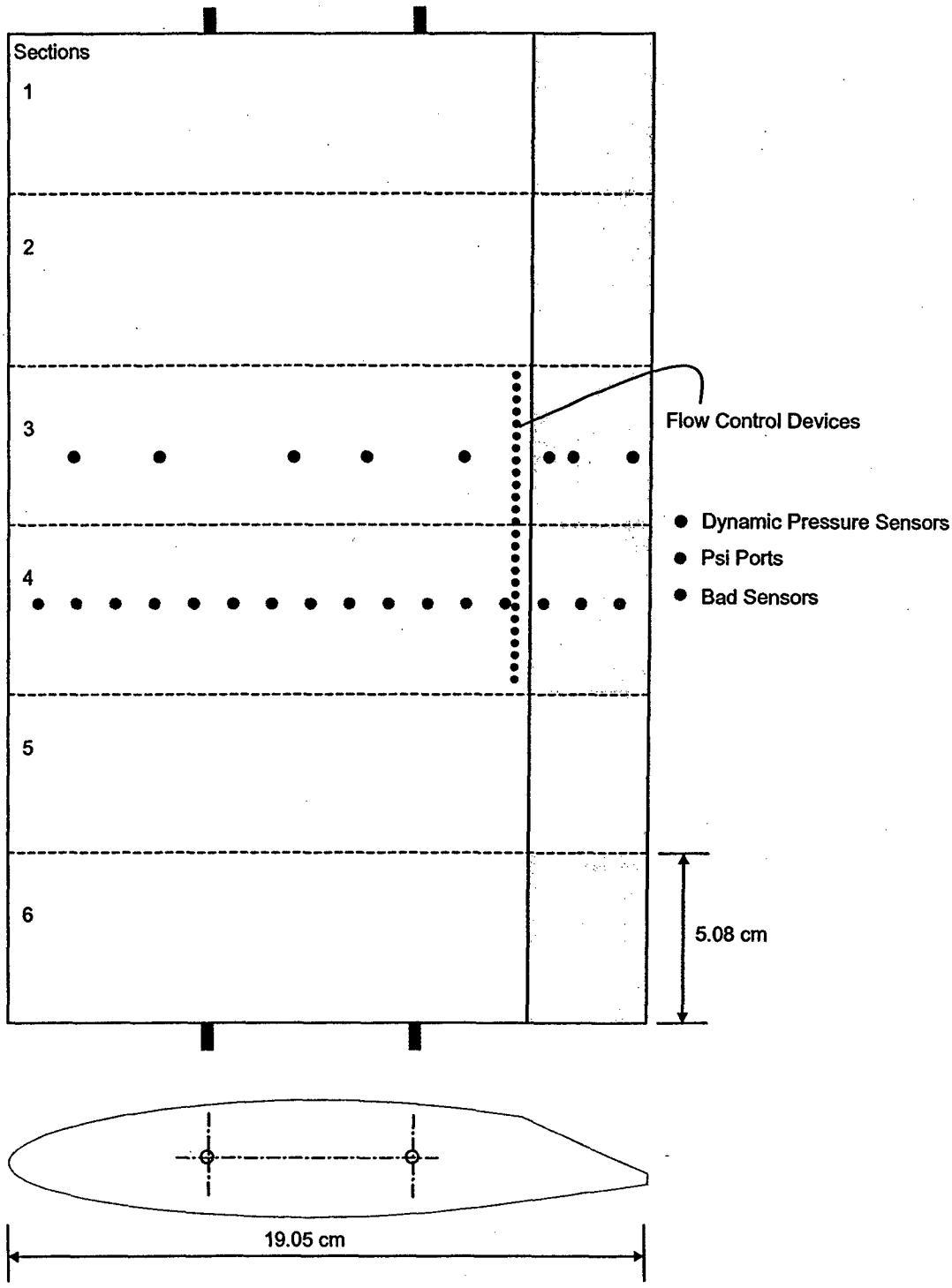

Fig. 1 Two-dimensional airfoil model with sensors and actuators on sections 3 and 4.

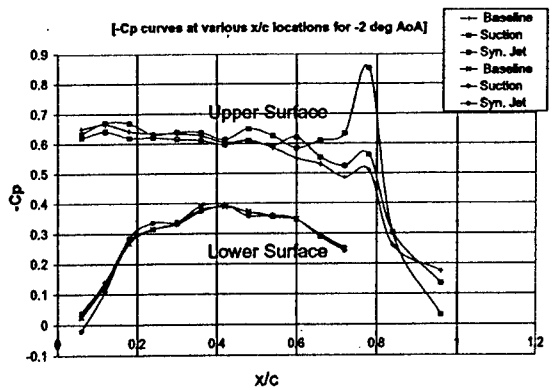

Fig. 2-a

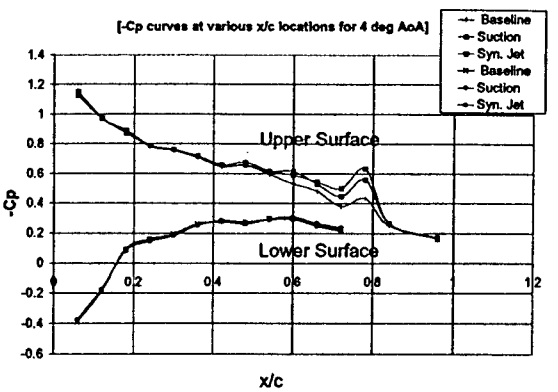

Fig. 2-d

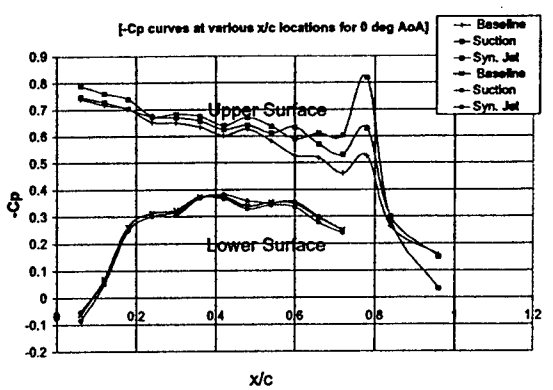

Fig. 2-b

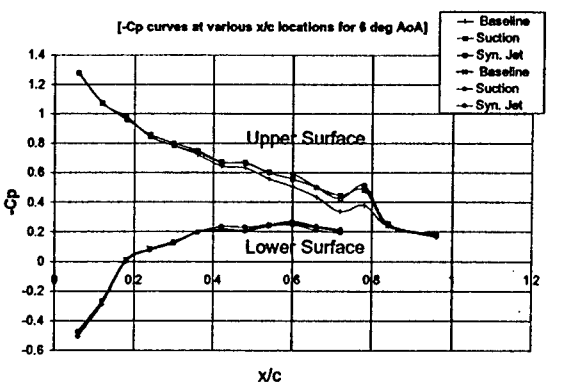

Fig. 2-e

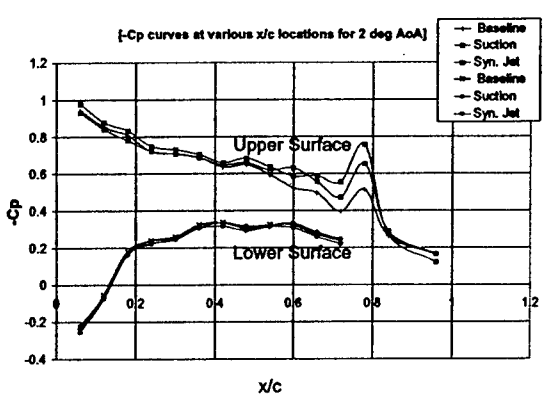

Fig. 2-c

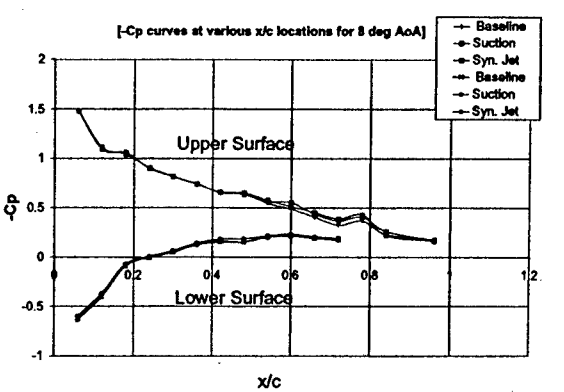

Fig. 2-f

Fig. 2 Effects of using zero-net mass synthetic jet and discrete suction on the pressure coefficient along the 2-D wing chord for different angles of attack.

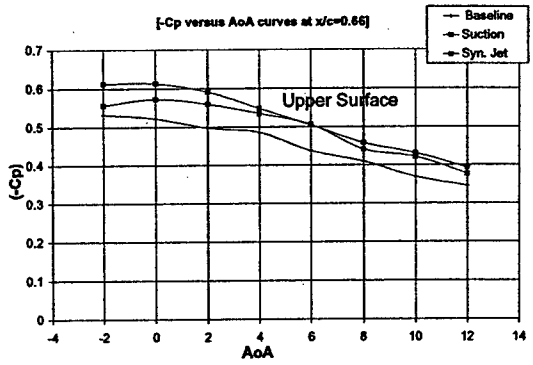

Fig. 3-a

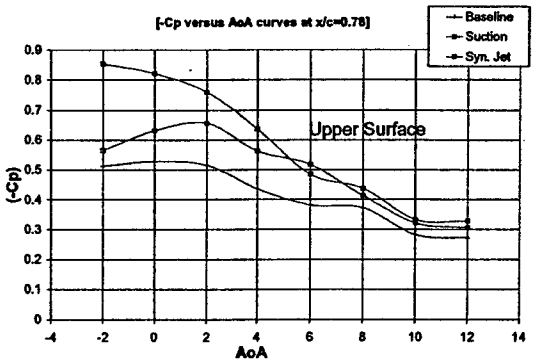

Fig. 3-c

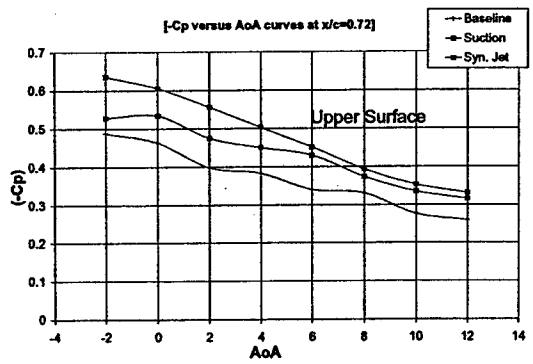

Fig. 3-b

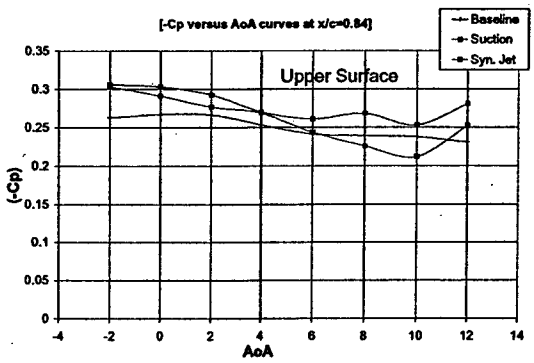

Fig. 3-d

Fig. 3 Effects of using zero-net mass synthetic jet and discrete suction on the pressure coefficient along the 2-D wing chord for different angles of attack at x/c=0.78

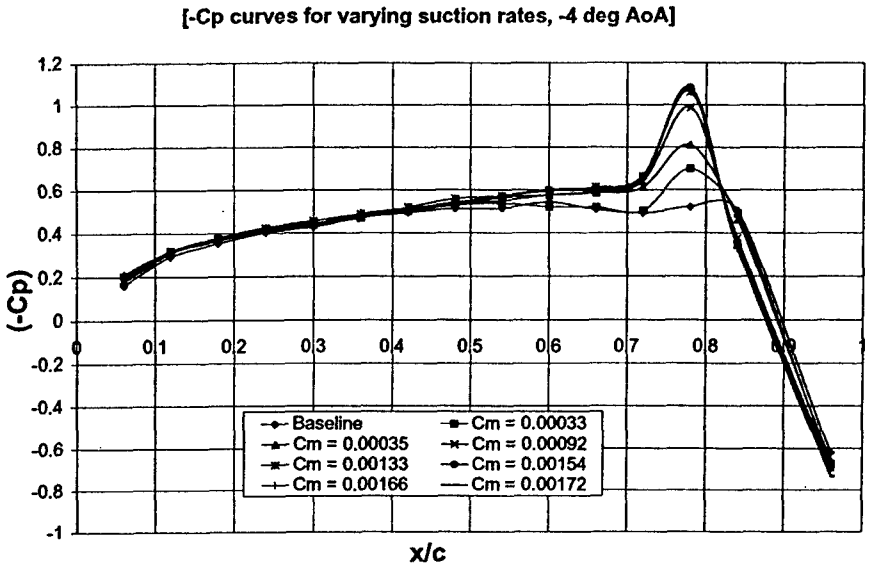

Fig. 4 Pressure coefficient along the wing chord for varying suction rates at -4° AoA (force modulation experiments).

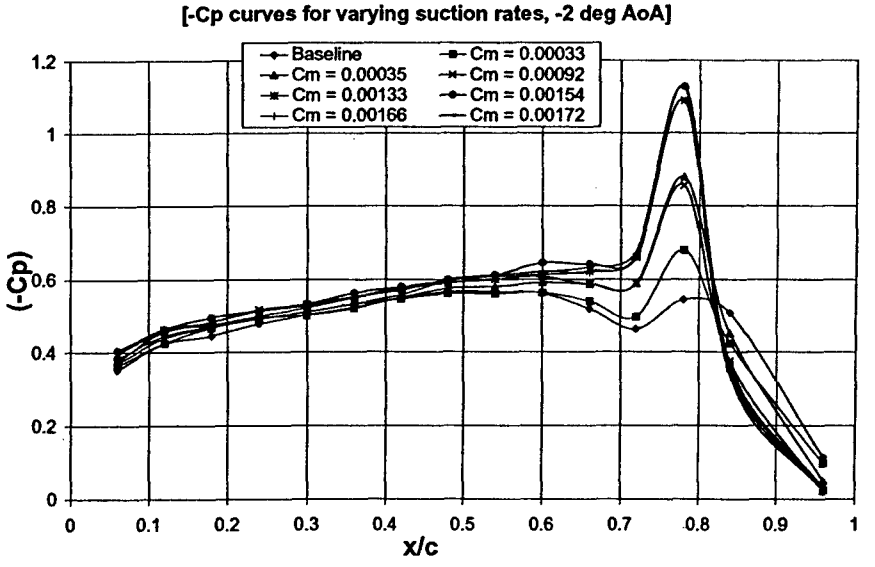

Fig. 5 Pressure coefficient along the wing chord for varying suction rates -2° AoA.(from force modulation experiments).

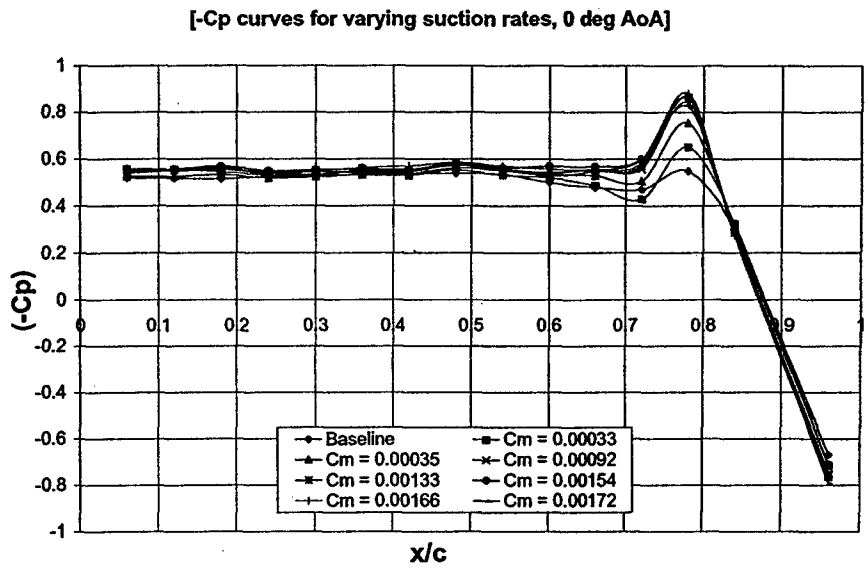

Fig. 6 Pressure coefficient along the wing chord for varying suction rates 0° AoA.(from force modulation experiments).

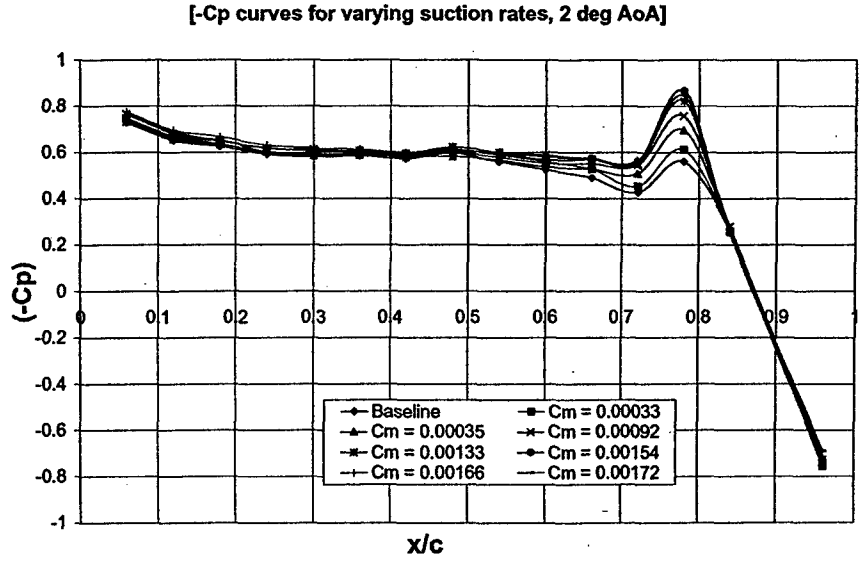

Fig. 7 Pressure coefficient along the wing chord for varying suction rates 2° AoA.(from force modulation experiments).

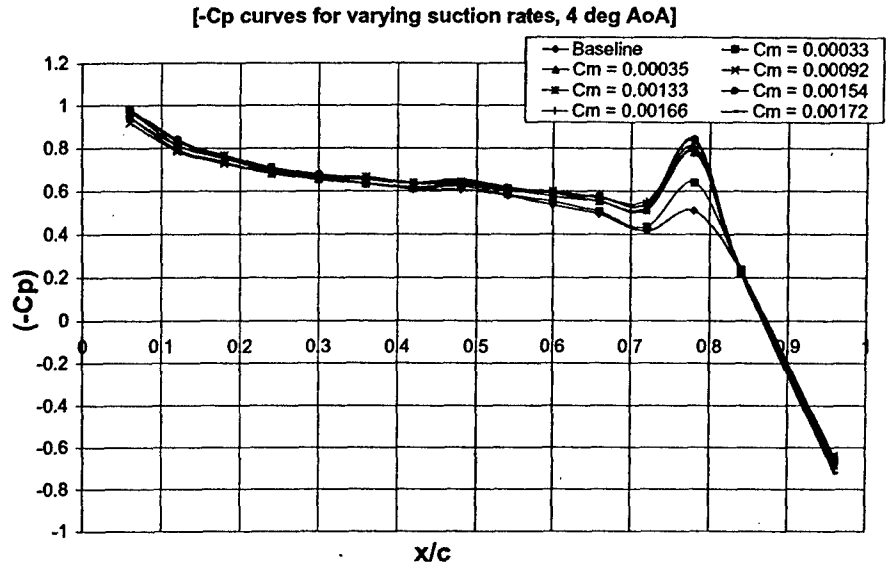

Fig. 8 Pressure coefficient along the wing chord for varying suction rates 4° AoA.(from force modulation experiments).

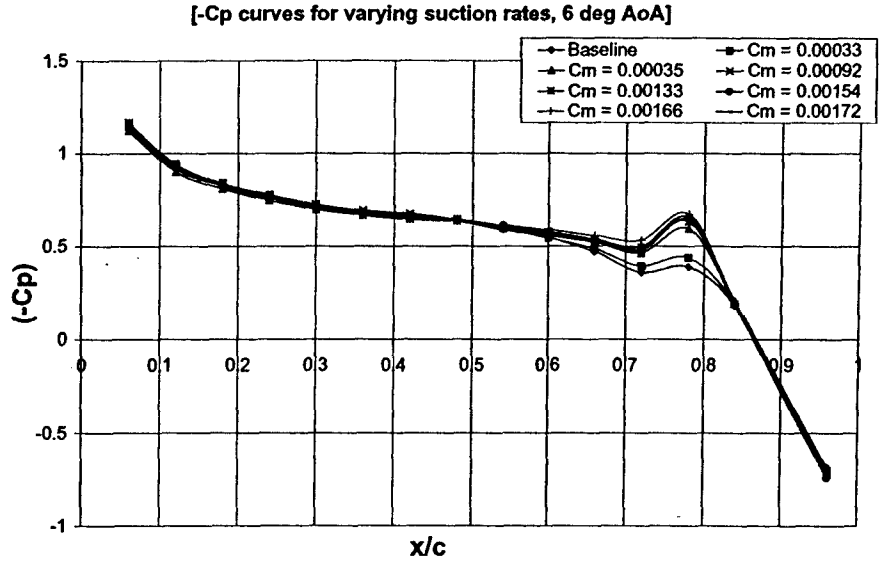

Fig. 9 Pressure coefficient along the wing chord for varying suction rates 6° AoA.(from force modulation experiments).

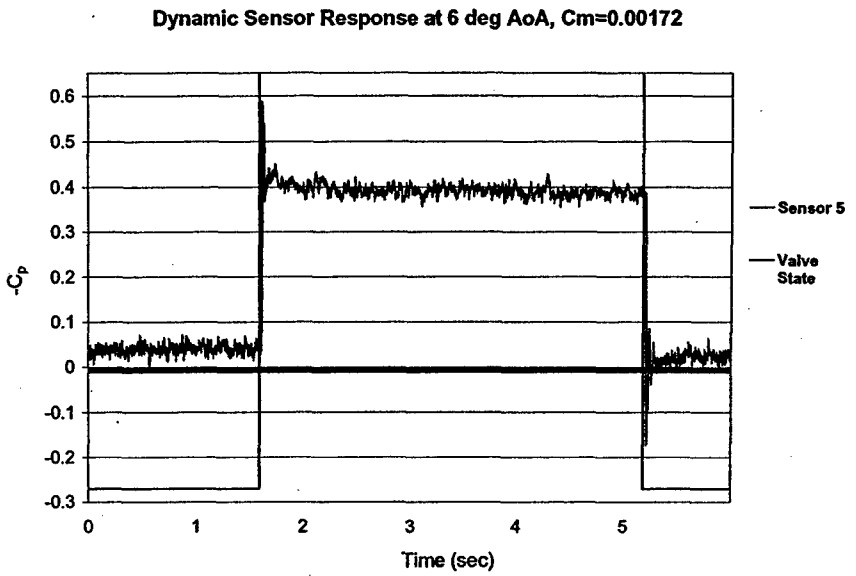

Fig. 10 Time history for the pressure coefficient to stabilize after the actuator-on/off state.

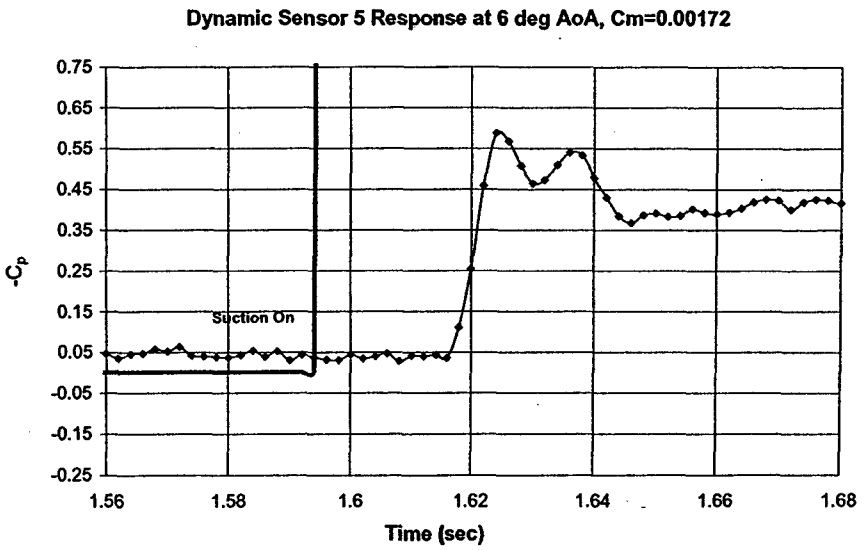

Fig. 11 Time history for the pressure coefficient to stabilize after the actuator-on state.

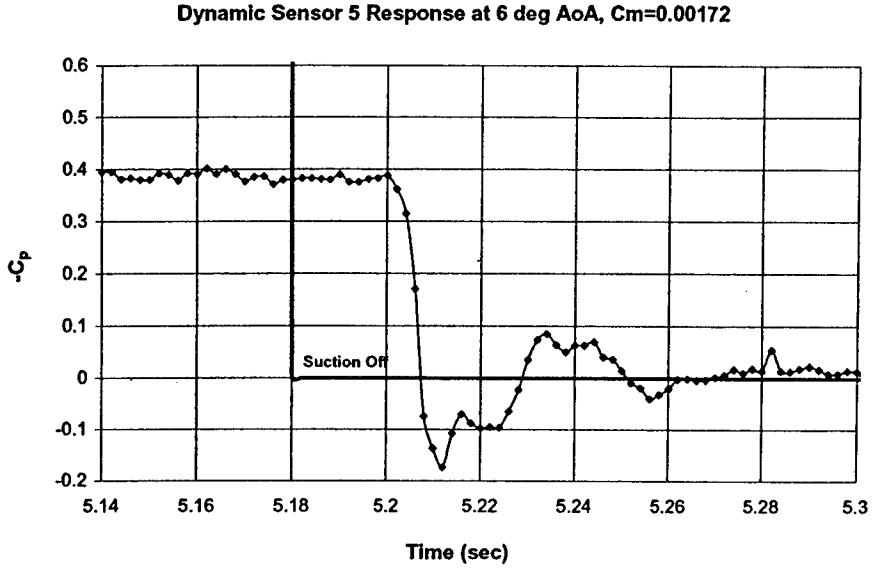

Fig. 12 Time history for the pressure coefficient to stabilize after the actuator-off state.

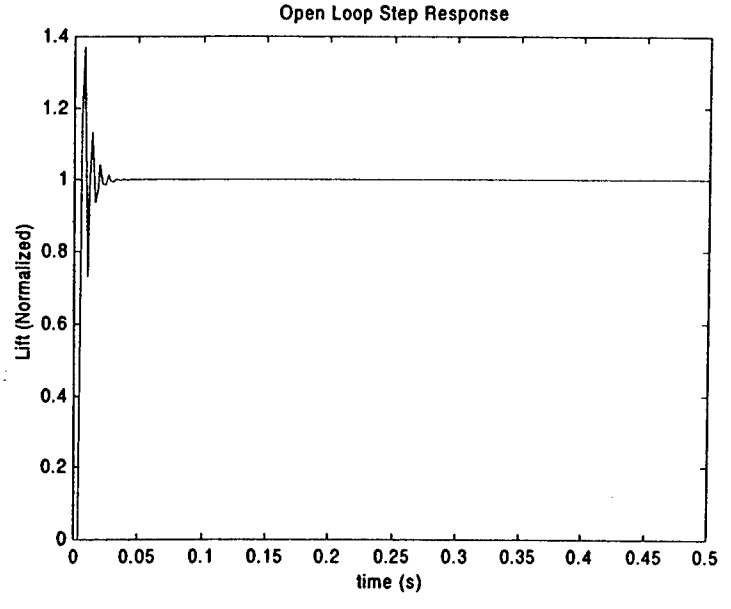

Fig. 13 Open-loop step response of the model.

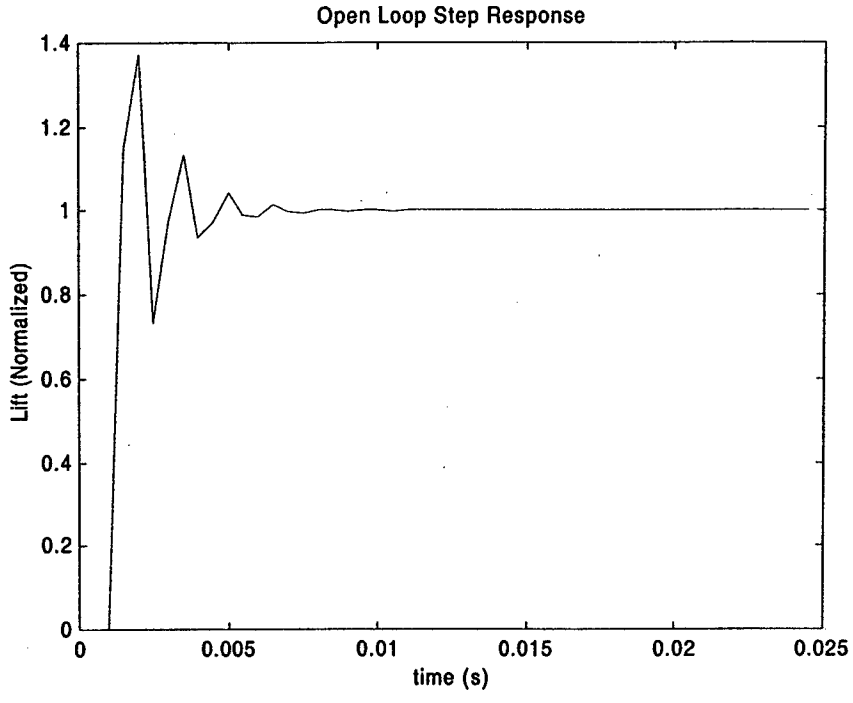

Fig. 14 Open-loop step response showing the delay in the model.

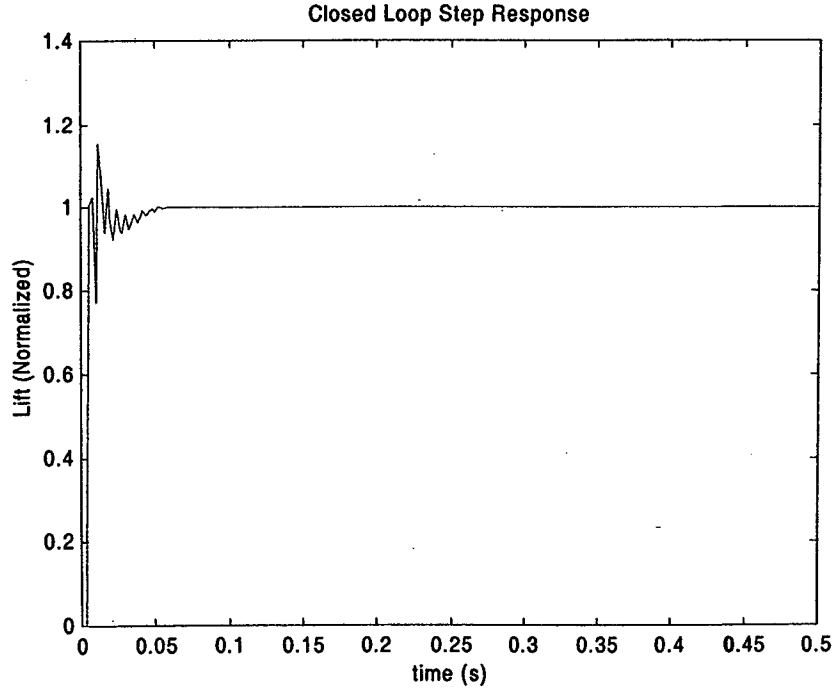

Fig. 15 Closed-loop step response of the model.

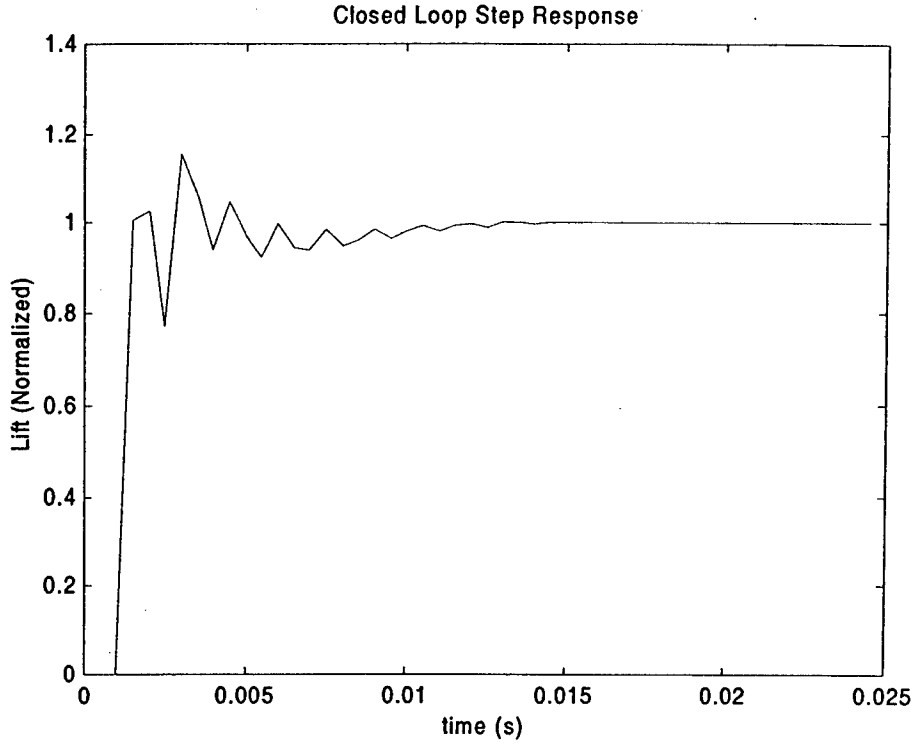

Fig. 16 Closed-loop step response showing delay in the model.

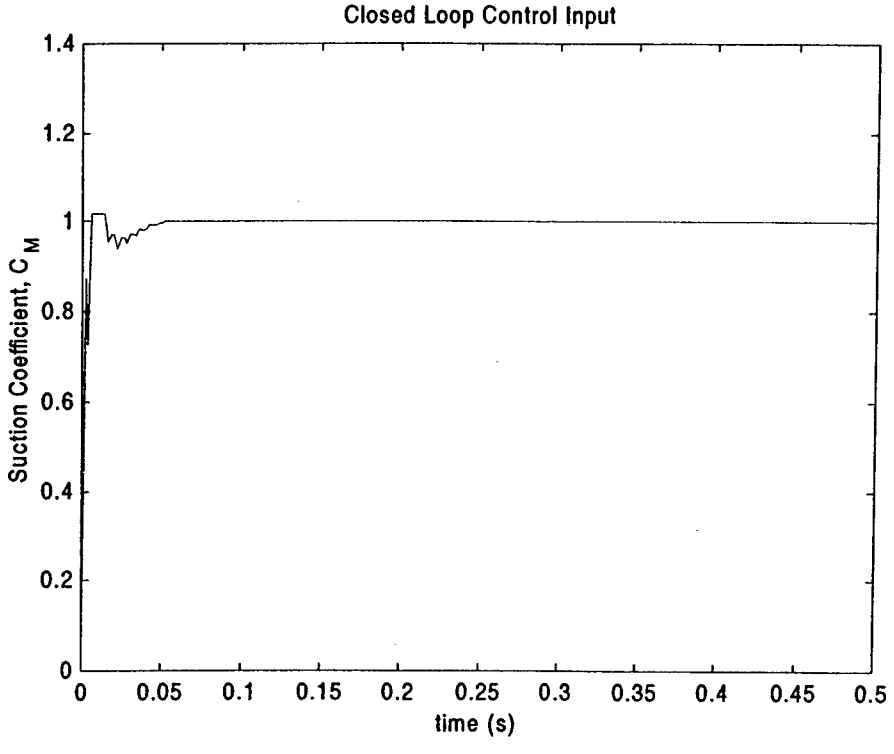

Fig. 17 Closed-loop control input to the system.

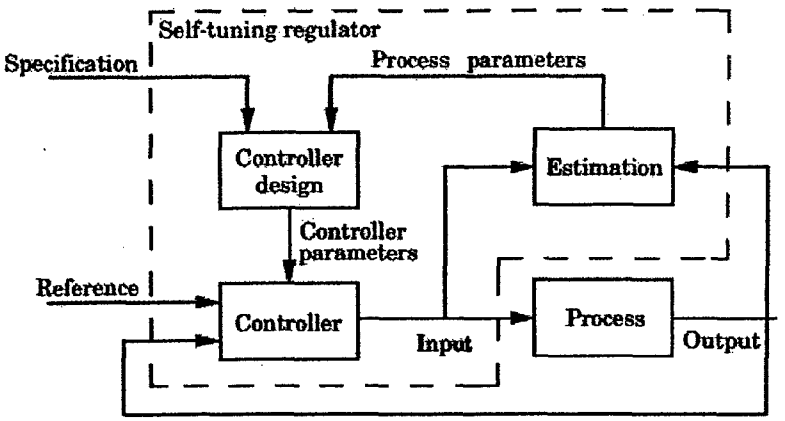

Fig. 18 Self Tuning Regulator (STR) Block Diagram.